ACS NANO

www.acsnano.org

ARTICLE

Efficient Scavenging of Solar and Wind Energies in a Smart City

Shuhua Wang,[†] Xue Wang,[†] Zhong Lin Wang,*[,†,‡] and Ya Yang*[,†]

[†]Beijing Institute of Nanoenergy and Nanosystems, Chinese Academy of Sciences, National Center for Nanoscience and Technology, Beijing 100083, P. R. China

[‡]School of Materials Science and Engineering, Georgia Institute of Technology, Atlanta, Georgia 30332-0245, United States

Supporting Information

ABSTRACT: To realize the sustainable energy supply in a smart city, it is essential to maximize energy scavenging from the city environments for achieving the self-powered functions of some intelligent devices and sensors. Although the solar energy can be well harvested by using existing technologies, the large amounts of wasted wind energy in the city cannot be effectively utilized since conventional wind turbine generators can only be installed in remote areas due to their large volumes and safety issues. Here, we rationally design a hybridized nanogenerator, including a solar cell (SC) and a triboelectric nanogenerator (TENG), that can individually/simultaneously scavenge solar and wind energies, which can be extensively installed on the roofs of the city buildings. Under the same device area of about 120 mm × 22 mm, the SC can deliver a largest output power of about 8 mW, while the output power of the TENG can be up to 26 mW. Impedance matching between the SC and TENG has been achieved by using a transformer to decrease the impedance of the TENG. The hybridized nanogenerator has a larger output current and a better charging performance than that of the individual SC or TENG. This research presents a feasible approach to maximize solar and wind energies scavenging from the city environments with the aim to realize some self-powered functions in smart city.

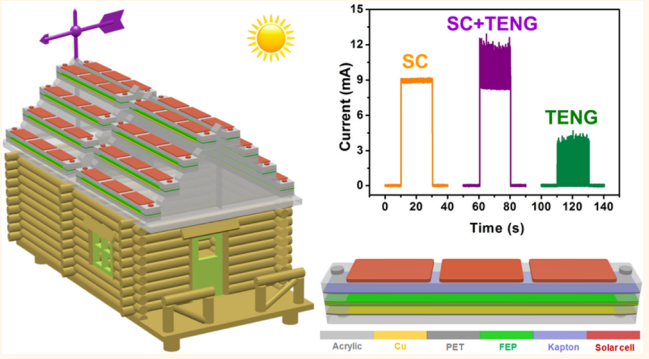

KEYWORDS: *triboelectric nanogenerator, solar cells, smart city, hybridized nanogenerator, Li-ion battery, self-powered*

A smart city is a city that can use intelligent devices to monitor/control all of the infrastructures and services in a sustainable and intelligent way.[1] The sustainable working of these intelligent devices requires a large energy consumption. Currently, the major approach for powering these devices is to use external power sources. The main drawback of the external power sources is that they require energy generation far away from the city and transportation to the city. Alternatively, using energy harvesters to scavenge energy from the city environments is an ideal solution to provide sustainable power sources for these intelligent devices. In the city environment, solar and wind energies are the major clean and renewable energy resources.[2,3] By integrating them with the city buildings, Si-based solar cells (SCs) have been utilized to scavenge solar energy.[4−6] For wind energy harvesting, conventional wind turbine generator systems can only be installed in remote areas due to their large volumes, safety issues, and high costs.[7−9] It is necessary to develop new wind energy harvesters that can be integrated with solar cells and extensively used in city buildings. In recent years, triboelectric nanogenerators (TENGs) based on coupling effects between triboelectric and electrostatic induction to scavenge mechanical energy have been attracting extensive attention owing to their small volume and low cost.[10−16] However, there has been no report about effectively integrating a SC and a TENG into a hybridized nanogenerator for scavenging solar and wind energies, which allows the large-scale installation in city buildings. It is highly desirable to develop this kind of energy-harvesting units to solve the power source issues of intelligent devices for realizing some self-powered functions in a smart city.

Here, we report a hybridized nanogenerator that consists of a SC and a TENG, which can be utilized to individually/simultaneously scavenge solar and wind energies. Under a device area of about 120 mm × 22 mm, the SC can deliver an output power of 8 mW, while the corresponding output power of the TENG can be up to 24 mW. A transformer has been utilized to decrease the impedance of the TENG for achieving the impedance matching between the SC and the TENG. As

Received: April 16, 2016
Accepted: May 5, 2016

DOI: 10.1021/acsnano.6b02575
ACS Nano XXXX, XXX, XXX−XXX

compared with the individual SC or TENG units, the hybridized nanogenerator has a larger output current and a better charging performance. Large-scale installation of the hybridized nanogenerators on the roofs of the city buildings can maximize solar and wind energies scavenging in city environments for realizing some self-powered functions in a smart city.

RESULTS AND DISCUSSION

Figure 1a illustrates a photograph of a traditional wind turbine generator, which has a large volume, a high cost, and obvious

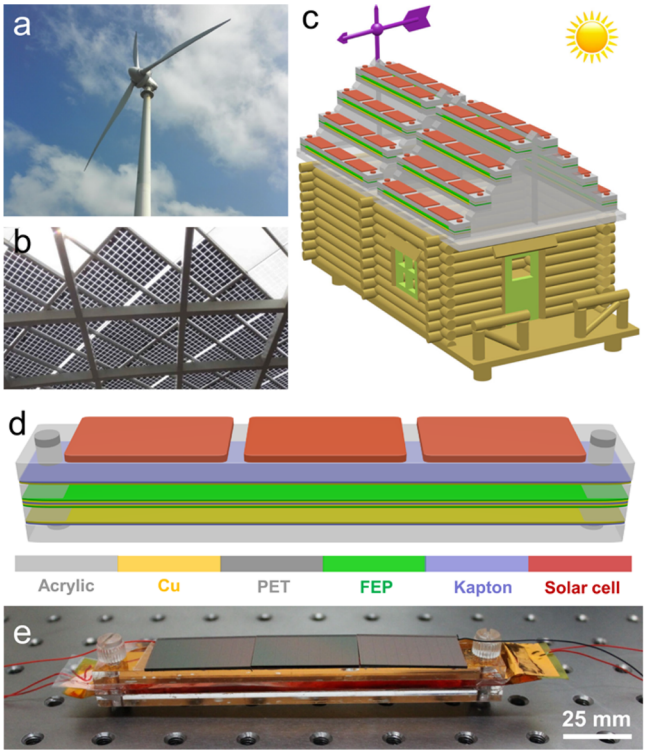

Figure 1. (a) Photograph of conventional wind turbine generator. (b) Photograph of the integrated SC units on the roof of a city building (c) Schematic diagram of the integrated hybridized nanogenerators on the roof of a house model. (d) Schematic diagram of the fabricated hybridized nanogenerator. (e) Photograph of the fabricated hybridized nanogenerator.

safety issues. Thus, this kind of wind energy harvesters can be only installed in remote areas. Figure 1b displays a photograph of integrated Si-based solar cells that have been installed on the roof of one city building. The traditional wind energy harvesters and the solar cells cannot be integrated due to the different device structures and working environments. To realize the scavenging of the solar and wind energies in city environments, we developed a hybridized nanogenerator that consists of a SC and a TENG, where this kind of hybridized nanogenerator allows large-scale installation on the roofs of city buildings, as depicted in Figure 1c. Figure 1d presents a schematic diagram of the detailed device structure, where a Si-based SC is fixed on the top of the TENG. The vibration film at the middle of TENG includes a Kapton film with two Cu electrodes on the both sides, where the FEP film as the triboelectric layer was affixed on the Cu electrode. Another two Cu electrodes were fixed on the top and bottom of the acrylic substrate, respectively, resulting in an air gap has been created between the two Cu electrodes.

The thickness of both the Kapton film and FEP film is about 25 μm, and the thickness of the Cu electrode is about 200 nm. The air gaps between the vibration film and the Cu electrode on the acrylic substrate are 2 mm, so that the height of air intake is about 4 mm. The SC unit has dimensions of 120 mm × 22 mm × 2 mm. Figure 1e displays a photograph of the fabricated hybridized nanogenerator, where the device has inner dimensions of ~120 mm × 22 mm × 4 mm. The working of the TENG is based on the wind-induced vibration of the middle Kapton/Cu/FEP films, resulting in the periodic contact and separation between the FEP and the top/bottom Cu film as both the conductive electrode and the triboelectric material.

Figure 2a depicts the output voltage of the TENG up to 375 V with a working frequency of about 160 Hz. The output

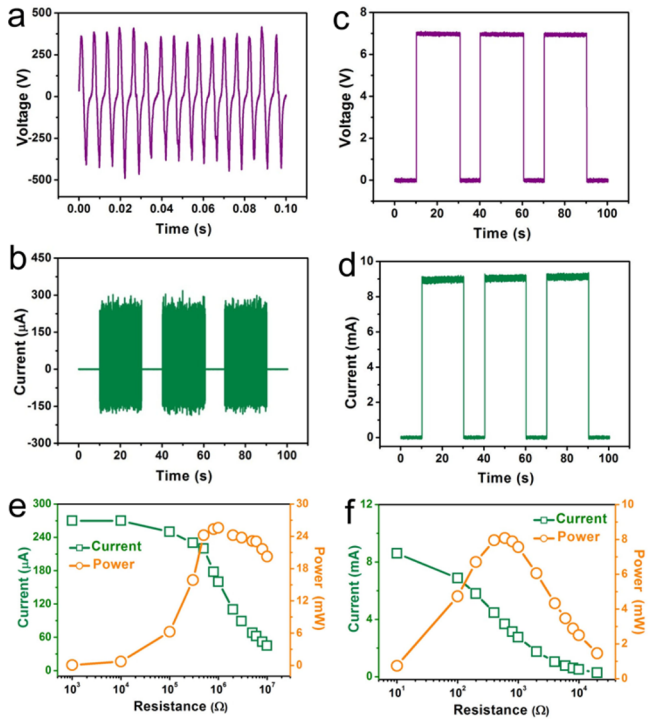

Figure 2. (a, b) Measured output voltage (a) and current (b) signals of the TENG under a wind speed of about 15 m/s. (c, d) Measured output voltage (c) and current (d) signals of the SC under a full-sun intensity. (e) Dependence of the output current and the corresponding output power of the TENG on the external loading resistances. (f) Dependence of the output current and the corresponding output power of the SC on the external loading resistances.

current of the TENG can reach 260 μA under a wind speed of about 15 m/s, as displayed in Figure 2b. The measured output voltage and current signals of the SC are about 7 V and 9 mA under a full-sun intensity (100 mW/cm^2), respectively, as illustrated in Figure 2c,d. As presented in Figure 2e, the output current of the TENG decreases with increasing the loading resistance, resulting in that the largest output power of the TENG can be up to 26 mW under the responding loading resistance of 1 MΩ. By measuring the change of current signals with different loading resistances, the largest output power of the SC is about 8 mW under a loading resistance of 600 Ω, as shown in Figure 2f. To solve the impedance matching issue between the TENG and the SC, a transformer has been utilized to decrease the impendence of the TENG. As displayed in

DOI: 10.1021/acsnano.6b02575
ACS Nano XXXX, XXX, XXX−XXX

Figure 3a,b, the output voltage of the TENG after using the transformer has been decreased to about 5 V, while the output current of the TENG after using the transformer can be increased to about 5 mA. By measuring the corresponding output current signals of the TENG after using the transformer under different loading resistances, we show in Figure 3c that the corresponding impedance of the TENG has been decreased from 1 MΩ to 600 Ω, where the largest output power is about 7 mW. After the impedance matching between the TENG and the SC has been achieved, the output current signals of the individual TENG, SC, and hybridized nanogenerator have been measured, as displayed in Figure 3d. It can be seen that the hybridized nanogenerator has the largest output current of about 12 mA as compared with that of the individual TENG or SC.

When the length and width of the TENG are fixed, the height of the air gap (the distance between the top and bottom Cu electrode) becomes the determining factor in affecting the output of the TENG. To obtain the largest output performance of the TENG, the systematic measurements were carried out through changing the height of the air gap, as described in Figure 3e. The possible reason for the largest output current under the height of 4 mm is associated with the optimized contact area between the vibration film and the top/bottom Cu electrode in the vibration process. The output current of the TENG increases with increasing the height of air gap at first and reaches the maximum value of 160 μA with the matched impedance of 1 MΩ, showing that the largest output power of the TENG can be up to 26 mW. As depicted in Figure 3f, the output powers of the TENG were measured under different wind flow directions. An obvious power decrease from 26 to 0 mW can be seen when the angle of wind direction changes from 0° to 40°, where the angle was defined as the angle between the wind flow and the length direction of the device. Figure 3g illustrates the output current stability of the TENG under the continuous operation of 1.21×10^7 cycles, indicating that a slow decrease of the output current in the first 9×10^6 cycles, and the output current then keeps a constant value of about 120 μA, where the cycle number of the TENG was calculated by utilizing both the working frequency and the continuous working time of the TENG.

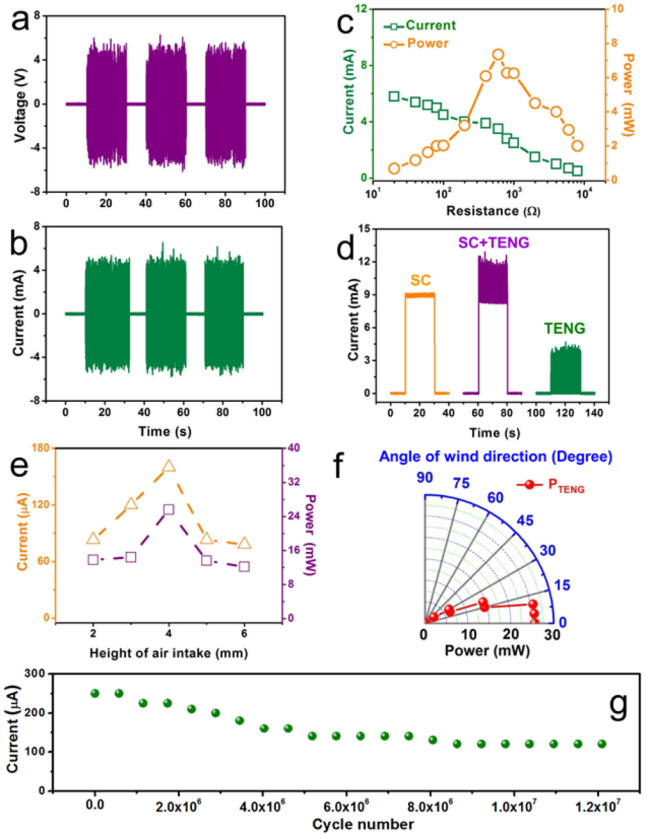

Figure 3. (a, b) Measured output voltage (a) and current (b) signals of the TENG after using a transformer. (c) Measured output current and calculated output power of the TENG after using a transformer under the different loading resistances. (d) Measured output current signals of the TENG, the SC, and the hybridized nanogenerator (SC+TENG). (e) Output current signals and the corresponding output power of the TENG under the different device heights. (f) Output power of the TENG depends on the different angles between the wind input and the direction of the device length ranged from 0° to 40°. (g) Measured output current stability of the TENG under continuous operations in 1.2×10^7 cycles at a wind speed of 15m/s.

A Li-ion battery was used to store energy generated by the hybridized nanogenerator. The battery developed in this work is based on the TiO_2 nanotube array as the electrode material. TiO_2 was grown on Ti foils by two-step anodization in ethylene glycol solution with subsequent annealing at 450 °C.[17,18] The XRD pattern (Figure S1) agrees well with the characteristic peaks of TiO_2, indicating that a purity phase was obtained. Figure 4a displays a scanning electron microscope (SEM)

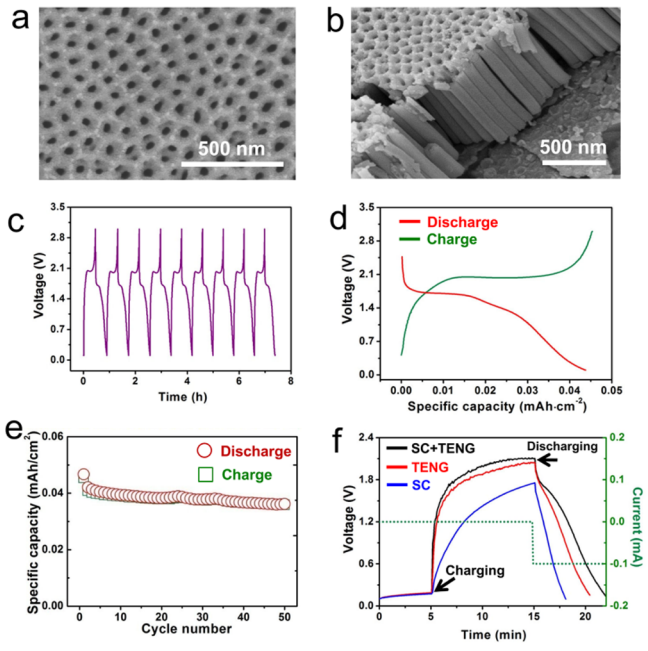

Figure 4. (a) SEM image of the as-grown TiO_2 nanotubes. (b) Cross-section SEM image of the TiO_2 nanotubes. (c) Charge and discharge voltage−time curves of the fabricated Li-ion battery under a constant current density of 0.1 mA/cm². (d) The first charge−discharge voltage profiles of the Li-ion battery. (e) Cycling performance of the Li-ion battery. (f) Measured charging and subsequent constant-current discharging curves of the Li-ion battery by using the TENG under a wind speed of 15 m/s, SC under an indoor light illumination, and the hybridized nanogenerator (TENG and SC), respectively.

DOI: 10.1021/acsnano.6b02575
ACS Nano XXXX, XXX, XXX−XXX

image of the TiO_2 nanotube array at the top view, where each TiO_2 nanotube has an inner diameter of about 100 nm and a wall thickness of about 50 nm. The length of the fabricated TiO_2 nanotube array is about 1 μm, as illustrated in Figure 4b. The TiO_2 nanotube array on the Ti substrate was cut into a square of 1 cm × 1 cm, which was used as an electrode material in lithium ion battery. Figure 4c,d exhibits the voltage profiles and the charge−discharge curves of the battery in which metal lithium was used as the counter electrode. A discharge capacity of 0.045 mAh/cm^2 can be obtained at a current density of 0.1 mA/cm^2.

Figure 4e displays a long-term cycling performance of the Li-ion battery with the charge and discharge currents of 0.1 mA, showing a good cycle stability. The fabricated battery can maintain its specific capacity of 0.04 mAh/cm^2 after 50 cycles. Figure 4f displays the charging and constant current-discharging performances of the Li-ion battery by using a TENG, an SC (under indoor illumination conditions), and a hybridized nanogenerator (TENG and SC), respectively. Under the same time conditions, the charging voltage of the hybridized nanogenerator is higher than that of individual TENG or SC, indicating that the hybridized nanogenerator has a better charging performance than that of the TENG or SC. As a result, the Li-ion battery can be charged from 0.2 to 2.1 V in 10 min by using the hybridized nanogenerator. Under a constant discharging current of 0.1 mA, the charged Li-ion battery can last for about 7 min to return to the original voltage, resulting in a total electrical capacity of about 11.7 μAh.

To demonstrate that the integrated hybridized nanogenerators can be installed on the roof of city buildings, four devices have been connected in parallel and installed on the roof of a house model, as illustrated in Figure S2. As displayed in Figure S3, the output current of the TENGs after using both a transformer and a rectifier circuit can be increased by increasing the integrated TENG number. One TENG can produce the output current of about 4.5 mA, while the integrated four TENGs can deliver the total output current of about 10.5 mA. A LED-array light in the house model was connected to the integrated hybridized nanogenerators. The SC cannot work under dark conditions, while the wind at night can drive the working of the TENG for solving the power source issues of some electronic devices. As displayed in Figure 5a,b, the LEDs-array light can be directly lighted by using the TENG to scavenge the wind energy for providing effective illumination in the house, which can be also seen in movie file 1. Usually, many kinds of sensors can be installed in a smart house. To demonstrate that the hybridized nanogenerators can scavenge the solar and wind energies from environments for powering some sensors, a temperature−humidity sensor was connected with a Li-ion battery that can be charged by the hybridized nanogenerators. The used Li-ion battery has a beginning voltage of about 0.8 V, which cannot drive the working of the temperature−humidity sensor. After the integrated four hybridized nanogenerators work simultaneously for scavenging the solar and wind energies in several seconds, the temperature−humidity sensor can be driven, as illustrated in Figure 5c. The temperature and humidity in the environment are about 25.1 °C and 23%, respectively, which can be also seen in movie file 2.

CONCLUSIONS

In summary, we have developed a hybridized nanogenerator, consisting of a SC and a TENG, that can individually/simultaneously scavenge solar and wind energies, which can be installed on the roofs of the city buildings in a large scale. Under the same device area of about 120 mm × 22 mm, the SC can deliver the largest output power of about 8 mW under a loading resistance of 600 Ω, while the output power of the TENG can be up to 26 mW under a loading resistance of 1 MΩ. By utilizing a transformer to decrease the impedance of the TENG, impedance matching between the SC and the TENG has been achieved. As compared with the individual SC or TENG, the hybridized nanogenerator has a better charging performance to charge a homemade Li-ion battery. Therefore, this research holds great promise for practical applications to maximize solar and wind energies scavenging from the environments in the city areas for realizing some self-powered functions in a smart city.

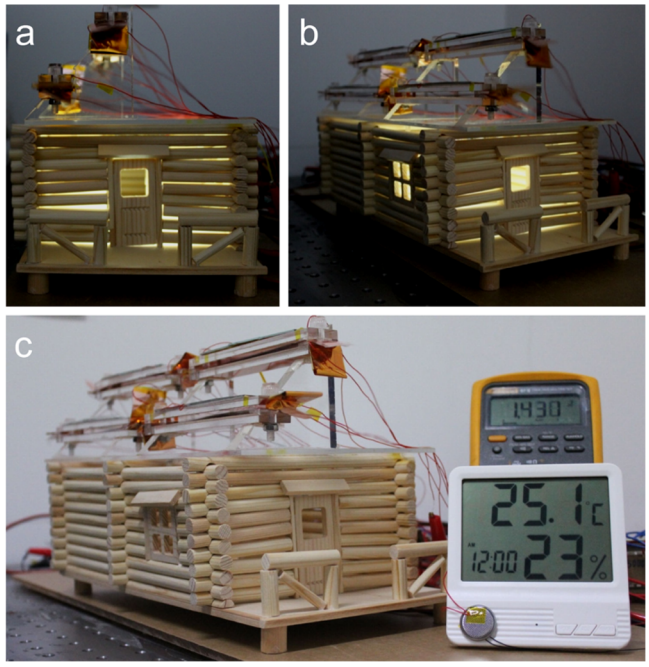

Figure 5. (a, b) Photographs of a LEDs-array light in the house model that can be lighted by using four integrated hybridized nanogenerators under the conditions of both the dark environment and a wind speed of ~15 m/s. (c) Photograph of a temperature−humidity sensor that can be powered by using the integrated four hybridized nanogenerators under conditions of both room-light illumination and a wind speed of ~15 m/s.

EXPERIMENTAL SECTION

Fabrication of the Hybridized Naongenerator. The fabricated device consists of a TENG and a SC, where a TENG includes a Kapton film with Cu electrodes and a FEP film affixing onto the Cu electrodes on both sides. There is a periodic contact and separation between the FEP film and Cu electrode on the acrylic substrate due to wind-induced vibration. Two acrylic sheets as the substrates of the Cu electrodes were cut by using a laser cutting machine. Two holes with a diameter of about 5 mm were fabricated at the both ends of the acrylic sheets. The supporting beams were fixed between two acrylic sheets. Screws were used to fix the two ends of the vibration film onto the supporting beam. The SC was fixed onto the top of the TENG, where the SC consists of many units in parallel and in series. The fabricated hybridized nanogenerator can individually/simultaneously scavenge solar and wind energies.

Fabrication of Li-ion Battery. Vertically aligned TiO_2 nanotubes were utilized as the electrode materials to fabricate a Li-ion battery, which were synthesized by an electrochemical anodization method. Ti

DOI: 10.1021/acsnano.6b02575
ACS Nano XXXX, XXX, XXX−XXX

metal foil (purity >99.9%) with a size of 8 cm × 2 cm × 0.1 mm was first heated at 300 °C for 30 min in a muffle furnace and then cleaned in ethanol for 30 min. The Ti foil samples were subsequently cleaned with deionized water by sonicating and then dried under N_2 conditions. In the first step, the experiment was carried out in ethylene glycol containing 0.3 wt % of NH_4F + 5 vol % of H_2O. The applied anodization voltage was about 50 V. After the sample was kept for 3 h, the Ti foil was then sonicated in H_2O_2 solution for 15 min to remove the anodized TiO_2 layer from the Ti substrate, which was then cleaned by using the deionized water and ethanol. Subsequently, a second-step of anodization was conducted at 50 V for the further growth of TiO_2 nanotubes. The second anodization time is about 10 min. All of the anodizing experiments were conducted in fresh electrolyte at room temperature. After anodization, the samples were cleaned with deionized water and then dried in oven at 80 °C. The as-prepared amorphous TiO_2 nanotube arrays were annealed in air at 450 °C for 2 h with a heating rate of 5 °C/min. An electrolyte of 1 M $LiPF_6$ in ethylene carbonate (EC) and dimethyl carbonate (DMC) (1:1 by volume) was utilized to fabricate the Li-ion battery. The Li-ion battery assembly was conducted in an Ar-filled glovebox with both O_2 and H_2O contents of less than 0.1 ppm.

Measurement of the Fabricated Device. The output current signals of the TENG were performed by a low-noise current preamplifier (Stanford Research SR570). The output voltage signals of the TENG were measured by a digital phosphor oscilloscope (Tektronix MDO 3024). The morphology of the prepared TiO_2 nanotube arrays was characterized by a scanning electron microscope (SEM, SUS8020). The crystalline phase of TiO_2 was analyzed by an X-ray diffractometer (Philips, Panalytical X'pert3, Cu Kα radiation source).

ASSOCIATED CONTENT

Supporting Information

The Supporting Information is available free of charge on the ACS Publications website at DOI: 10.1021/acsnano.6b02575.

XRD pattern, photograph of the nanogenerators, and measured output current signals (PDF)

Movie file of harvesting wind energy in dark conditions for powering an LED-array light in the wooden house model (AVI)

Movie file of harvesting wind and light energies to sustainably power a digital temperature−humidity sensor (AVI)

AUTHOR INFORMATION

Corresponding Authors

*(Prof. Ya Yang) E-mail: yayang@binn.cas.cn.

*(Prof. Zhong Lin Wang) E-mail: zlwang@gatech.edu.

Notes

The authors declare no competing financial interest.

ACKNOWLEDGMENTS

This work was supported by the Beijing Natural Science Foundation (2154059), the National Natural Science Foundation of China (Grant Nos. 51472055 and 61404034), External Cooperation Program of BIC, Chinese Academy of Sciences (Grant No. 121411KYS820150028), the 2015 Annual Beijing Talents Fund (Grant No. 2015000021223ZK32), and the "Thousands Talents" Program for the Pioneer Researcher and His Innovation Team, China. The corresponding patent has been submitted based on the research presented here.

REFERENCES

(1) Giffinger, R.; Fertner, C.; Kramar, H.; Kalasek, R. *Smart Cities: Ranking of European Medium-Sized Cities*; Centre of Regional Science: Vienna, 2007.

(2) Gupta, N. A Review on the Inclusion of Wind Generation in Power System Studies. *Renewable Sustainable Energy Rev.* **2016**, *59*, 530−543.

(3) Li, K.; Bian, H.; Liu, C.; Zhang, D.; Yang, Y. Comparison of Geothermal with Solar and Wind Power Generation Systems. *Renewable Sustainable Energy Rev.* **2015**, *42*, 1464−1474.

(4) Fan, Z.; Javey, A. Solar Cells on Curtains. *Nat. Mater.* **2008**, *7*, 835−836.

(5) Jeong, S.; Garnett, E. C.; Wang, S.; Yu, Z.; Fan, S.; Brongersma, M. L.; McGehee, M. D.; Cui, Y. Hybrid Silicon Nanocone-Polymer Solar Cells. *Nano Lett.* **2012**, *12*, 2971−2976.

(6) Jeong, S.; McGehee, M. D.; Cui, Y. All-Back-Contact Ultra-Thin Silicon Nanocone Solar Cells with 13.7% Power Conversion Efficiency. *Nat. Commun.* **2013**, *4*, 2950.

(7) Shupe, J. W. Energy Self-Sufficiency for Hawaii. *Science* **1982**, *216*, 1193−1199.

(8) Marshall, C. W. Power and Energy from the Winds. *Nature* **1956**, *117*, 1050−1051.

(9) Morse, J. G. Energy for Remote Areas. *Science* **1963**, *139*, 1175−1180.

(10) Chun, J.; Kim, J. W.; Jung, W.; Kang, C.-Y.; Kim, S.-W.; Wang, Z. L.; Baik, J. M. Mesoporous Papers Impreganted with Au Nanoparticles as Effective Dielectrics for Enhancing Triboelectric Nanogenerator Performance in Harsh Environments. *Energy Environ. Sci.* **2015**, *8*, 3006−3012.

(11) Guo, H.; Chen, J.; Tian, L.; Leng, Q.; Xi, Y.; Hu, C. Airflow-Induced Triboelectric Nanogenerator as a Self-Powered Sensor for Detecting Humidity and Airflow Rate. *ACS Appl. Mater. Interfaces* **2014**, *6*, 17184−9.

(12) Chung, J.; Lee, S.; Yong, H.; Moon, H.; Choi, D.; Lee, S. Self-Packing Elastic Bellows-Type Triboelectric Nanogenerator. *Nano Energy* **2016**, *20*, 84−93.

(13) Seol, M.-L.; Woo, J.-H.; Jeon, S. B.; Kim, D.; Park, S. J.; Hur, J.; Choi, Y.-K. Vertically Stacked Thin Triboelectric Nanogenerator for Wind Energy Harvesting. *Nano Energy* **2015**, *14*, 201−208.

(14) Wang, S.; Mu, X.; Wang, X.; Gu, A. Y.; Wang, Z. L.; Yang, Y. Elasto-Aerodynamics-Driven Triboelectric Nanogenerator for Scavenging Air-Flow Energy. *ACS Nano* **2015**, *9*, 9554−9563.

(15) Zhang, L.; Zhang, B.; Chen, J.; Jin, L.; Deng, W.; Tang, J.; Zhang, H.; Pan, H.; Zhu, M.; Yang, W.; Wang, Z. L. Lawn Structured Triboelectric Nanogenerators for Scavenging Sweeping Wind Energy on Rooftops. *Adv. Mater.* **2016**, *28*, 1650−1656.

(16) Wang, Z. L.; Chen, J.; Lin, L. Progress in Triboelectric Nanogenerators as a New Energy Technology and Self-Powered Sensors. *Energy Environ. Sci.* **2015**, *8*, 2250−2282.

(17) Li, Z.; Ding, Y.; Kang, W.; Li, C.; Lin, D.; Wang, X.; Chen, Z.; Wu, M.; Pan, D. Reduction Mechanism and Capacitive Properties of Highly Electrochemically Reduced TiO_2 Nanotube Arrays. *Electrochim. Acta* **2015**, *161*, 40−47.

(18) Zheng, D.; Lv, M.; Wang, S.; Guo, W.; Sun, L.; Lin, C. A Combined TiO_2 Structure with Nanotubes and Nanoparticles for Improving Photoconversion Efficiency in Dye-Sensitized Solar Cells. *Electrochim. Acta* **2012**, *83*, 155−159.

DOI: 10.1021/acsnano.6b02575
ACS Nano XXXX, XXX, XXX−XXX